Structure and Function in the Isolated Reaction Center Complex of Photosystem II. 1. Ultrafast Fluorescence Measurements of PSII

Brent Donovan,[†] Larry A. Walker II,[†] Daniel Kaplan,[§] Marcel Bouvier,[⊥] Charles F. Yocum,[†,||] and Roseanne J. Sension*[,†,‡]

Department of Chemistry, Department of Biology, and Center for Ultrafast Optical Science, University of Michigan, Ann Arbor, Michigan 48109, MEDOX ELECTRO-OPTICS, 3940 Varsity Drive, Ann Arbor, Michigan 48108, and Alliage, 77 rue de Cardinal Lemoine, 75005 Paris, France

Received: March 28, 1997[⊗]

Time-resolved fluorescence measurements of PSII D1−D2−Cytb559 reaction center complexes were made by using an optical signal analyzer based on a streak camera tube synchronized with subpicosecond jitter to a femtosecond 1 kHz titanium:sapphire laser system. The instrumental response function of this analyzer was 4−4.5 ps fwhm under experimental conditions. Synchronization permitted extensive signal averaging and allowed measurements to be made with low incident pulse energy (3−10 nJ) and photon flux ((1.5−5.0) $\times$ 10^{13} photons/cm^2). Fluorescence decays were obtained following excitation throughout the Q_y band of PSII. The data are inconsistent with an effective or apparent charge separation time scale of ca. 3 ps following direct excitation of P680. Rather, the effective charge separation from a quasi-equilibrium of chromophore excited states is either quite fast ($\leq$1.25 ps) or relatively slow ($\geq$20 ps). The most consistent interpretation of the available data involves rapid energy redistribution processes within pools of pigments, somewhat slower energy redistribution between pools of pigments, and relatively slow multiexponential charge separation.

Introduction

Considerable effort has been expended in recent years to elucidate the mechanism of energy transfer and charge separation in the photosystem II (PSII) reaction center of green plants. The PSII protein complex is responsible for trapping light energy to provide the oxidation potential required to split water and produce molecular oxygen. Ultrafast spectroscopic techniques have been used extensively to investigate the primary electron transfer and energy transfer processes in PSII. Transient absorption measurements, particularly in the Q_y region of chlorophyll a (Chl) between 660 and 690 nm and the Q_x region of pheophytin a (Pheo) at ca. 545 nm, exhibit decays and growths that range in time scale from $\leq$100 fs to >100 ps.[1−4] Picosecond fluorescence measurements demonstrate a slow overall decay of the excited state population in PSII due to charge recombination fluorescence.[5−7] This decay is modestly dependent upon the excitation wavelength.

The general model emerging from the transient absorption and fluorescence measurements is characterized by the lack of an effectively unidirectional energy transfer or electron transfer trap in PSII prior to the secondary electron transfer from the Pheo to the plastoquinone (Q). (See for example discussion in ref 7.) The specific models for energy transfer and electron transfer in PSII are still controversial, however. Data from transient absorption alone are often ambiguous due to overlapping contributions from ground state bleaching, stimulated emission, and imperfectly determined excited state and photoproduct absorption signals. Most transient absorption measurements have concentrated on changes in the Q_y region of the spectrum, where the complications introduced by spectral congestion and also by competing absorption, bleaching, and stimulated emission contributions are particularly acute.[8] Transient absorption measurements have also been used extensively to investigate the bleaching dynamics of the Pheo Q_x band at 545 nm.[1−4,8] Stimulated emission does not contribute to the signal in this wavelength region. In addition, spectral measurements may be used to separate the broad excited state and photoproduct absorption signals from the bleaching of the relatively narrow Pheo Q_x band. However, these measurements cannot distinguish between loss of Pheo ground state population due to production of the ion pair state and loss of population due to the formation of electronically excited Pheo. Interpretation of the transient absorption data may be facilitated by the acquisition of spontaneous emission kinetics which probe only the population of the emitting state(s).

Heretofore, fluorescence measurements on PSII reaction centers have been limited to detection systems having ca. 20−30 ps instrument functions (full width at half-maximum, fwhm). In particular, a streak camera with ca. 18 ps resolution was used to investigate the fluorescence decay in PSII.[6] However, the use of nonspecific excitation at 590 nm limits the usefulness of these measurements in the analysis of the early time behavior of electronically excited PSII. Additionally, an extensive time-correlated single photon counting (TCSPC) analysis has been carried out with an intrinsic instrument function of ca. 30 ps.[7] Deconvolution procedures allow precise determination of time constants considerably shorter than the instrumental fwhm, especially with the high signal-to-noise ratio available with the TCSPC method. However, the absolute numerical reliability of deconvolution may be questioned when the time constants being considered approach widths of one or two data points or ca. 10% of the instrumental fwhm. As critical decay components of 1−4 ps are proposed in PSII, response functions of less than 5 ps are desirable. Fluorescence up-conversion measurements of PSII, capable of subpicosecond time resolution, are hindered by the additional requirement of low photon flux, which is necessary if complications due to multiply excited reaction center complexes are to be avoided.[4,9]

* To whom correspondence should be addressed.
[†] Department of Chemistry, University of Michigan.
[‡] Center for Ultrafast Optical Science, University of Michigan.
[§] Alliage.
[⊥] MEDOX ELECTRO-OPTICS.
[||] Department of Biology, University of Michigan.
[⊗] Abstract published in *Advance ACS Abstracts,* June 1, 1997.

S1089-5647(97)01112-7 CCC: $14.00

In this paper we report time-resolved fluorescence measurements of PSII D1−D2−Cyt b559 reaction center (RC) complexes. Measurements were made by using an optical signal analyzer based on a streak camera tube synchronized with subpicosecond jitter to a femtosecond Ti:sapphire laser system. The instrumental response function of this analyzer was 4.5 ps fwhm under experimental conditions. The sensitivity of the detection system and the ability to signal average allowed analysis of fluorescence kinetics following excitation with 3−10 nJ pulses.

The present data are inconsistent with an effective or apparent charge separation time scale of ca. 3 ps following direct excitation of P680. No population decay component in the 2−4 ps range is observed for any combination of excitation and emission wavelengths. Rather, the effective charge separation from a quasi-equilibrium of chromophore excited states is either quite fast ($\leq$1.25 ps) or relatively slow ($\geq$20 ps). The most consistent interpretation of the available data invokes rapid energy redistribution processes within pools of pigments, somewhat slower energy redistribution between pools of pigments, and relatively slow multiexponential charge separation from a progressive quasi-equilibrium of pigment excited states. Such a model may be consistent with an intrinsic charge separation time scale of ca. 3 ps.

Experimental Section

PSII CP47−D1−D2−Cyt b559 reaction center complexes were isolated from spinach[4,10−12] and used as the starting material for the RC complex prepared according to ref 12 with slight modifications. All experiments were performed under anaerobic conditions created by addition of catalase, glucose, and glucose oxidase.[13] The sample was kept on ice in a small reservoir and flowed through a 2 mm fluorescence cell. This maintained the sample temperature well below ambient. The absorbance of the sample was 0.95 to 1 at the Q_y maximum (675.5 nm) in the 2 mm cell. The D1−D2−Cyt b559 complexes were periodically changed to ensure that they did not degrade due to prolonged exposure to the pump laser light. This was very important in the present fluorescence measurements as sample degradation led to the appearance of a substantial scattering component which could not always be eliminated by spectral filtering. As the sample aged, the amount of scattering increased rapidly, apparently due to protein aggregation. No change was detected in the first 30 min, but after 60 min the sample exhibited a clear increase in the scattering component.

A regeneratively amplified Ti:sapphire laser system was used to produce ca. 70 fs pulses at 800 nm with a 1 kHz repetition rate. This beam was split, and half of the beam was used to produce tunable pulses in a home-built optical parametric amplifier (OPA). The excitation pulses produced by the OPA ranged from 656 to 690 nm. The other half of the Ti:sapphire laser beam was used as a reference to synchronize the optical signal analyzer. A 10 nm band-pass interference filter centered at the indicated detection wavelength was used to filter the fluorescence and exclude scattered laser light from the camera.

To minimize nonlinear effects, specifically singlet−singlet annihilation, the intensity of the excitation beam was 3−10 nJ/pulse ($(1-3.5)\times10^{10}$ photons/pulse), focused to a diameter of 300 μm. The photon flux at the top of the sample was therefore $(1.5-5)\times10^{13}$ photons/cm^2 per pulse. The use of such a low photon flux essentially eliminates annihilation processes by exciting an average of 0.05−0.20 pigments per reaction center.[9]

For the present set of measurements, the excitation beam, propagating in the *y*-direction and polarized in the *x*-direction, was focused inside the front window of a quartz fluorescence cell (Figure 1). The total fluorescence propagating in the *z*-direction was collected and imaged onto a streak camera tube. This geometry leads to the presence of anisotropy and population decay in the signal. The total signal due to population change is obtained from

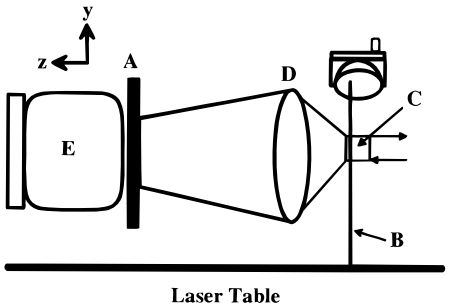

Figure 1. Schematic diagram of the experimental setup for fluorescence measurements. A 10 nm band-pass interference filter (A) was used to exclude scattered laser light from the camera. The excitation beam (B), propagating in the *y*-direction and polarized in the *x*-direction, was focused inside the front window of the 2 mm square fluorescence flow cell (C). The total fluorescence propagating in the *z*-direction (D) was collected and imaged onto a streak camera (E).

$$P(t) = S_X(t) + S_Y(t) + S_Z(t) = S_{||}(t) + 2S_{\perp}(t) \qquad (1)$$

while the measured signal is

$$S_{meas}(t) = S_X(t) + S_Y(t) = S_{||}(t) + S_{\perp}(t) \qquad (2)$$

The anisotropy as a function of time is defined by

$$r(t) = \frac{S_{||}(t) - S_{\perp}(t)}{S_{||}(t) + 2S_{\perp}(t)} \qquad (3)$$

The measured signal $S_{meas}(t)$ can be related to the population and anisotropy signals:

$$S_{meas}(t) = S_{||}(t) + S_{\perp}(t) = (P(t)/3)(2 + r(t)) \qquad (4)$$

The anisotropy decay contribution to the fluorescence may be estimated by using transient absorption measurements made with pump and probe wavelengths throughout the Q_y absorption band.[14,15] For excitation at 670 and 680 nm the absorption anisotropy signals are dominated by a fast (ca. 200 fs) anisotropy decay from 0.4 to 0.15−0.10. All other decay components are much slower and of small amplitude ($\Delta r < 0.1$). For the other two relevant wavelength combinations, 690 nm excitation with 670 nm detection and 660 nm excitation with 690 nm detection, the anisotropy contributions to the transient absorption are of smaller amplitude. For all combinations of pump and probe wavelengths used in transient absorption (excitation 660, 670, 680, and 690 nm; probe 670, 680, and 690 nm), the anisotropy reaches a plateau between 0.10 and 0.03 and is essentially flat from 5 to 50 ps.[15] It is reasonable to assume that the fluorescence will contain an anisotropy decay dominated by energy transfer processes similar to that observed in the transient absorption measurement (i.e., a rapid decay of large amplitude followed by a nearly constant plateau). The fluorescence data obtained in the present set of measurements should therefore be perturbed minimally by anisotropy contributions.

For excitation at 670 and 680 nm and detection at 690 and 691 nm with a 4.5 ps instrument function, a fast anisotropy decay is included in the analysis of the fluorescence data by using eq 3 to fit the data with $r(t) = 0.27e^{-t/200fs} + 0.13$. No anisotropy decay is included in the analysis of the other data

sets. The correction for anisotropy decay changes the magnitude and time constant for the fastest population decay component slightly but does not alter any of the conclusions presented.

The streak camera tube is part of a system provided by MEDOX ELECTRO-OPTICS, which includes a photoconductor driven, high-voltage sweep circuit to precisely synchronize the detection time window to the incoming laser pulse. This synchronization permits the integration of successive signals from the 1 kHz train, thus improving sensitivity compared to a single shot streak camera. The photoconductor was activated by the reference beam which was properly time-shifted using an optical delay line. The fluorescence is imaged onto the photocathode of the streak camera. The resulting width of the line is 0.15−0.30 mm, 3−6 times the spatial resolution of the camera tube. The electron beam is swept synchronously in the horizontal direction perpendicular to the vertical line image. The signal is detected by a CCD. Integration of successive images is performed in analog mode inside the CCD circuit and numerically after read out.

The ultimate time resolution was limited by several factors. The jitter between successive measurements corresponded to a standard deviation of 0.7 ps.[16] Spatial broadening related to finite image size, time broadening due to intrinsic limitations of the streak tube, and optical delays in the finite horizontal and vertical dimensions of the image also contribute to the overall temporal resolution of the instrument. A fwhm of 4−4.5 ps was observed for laser scatter (pulse width ca. 200 fs) imaged onto the streak camera with a streak voltage of 800 V under the present experimental conditions. A slightly different camera configuration resulted in a 5−9 ps fwhm for laser scatter imaged onto the streak camera with a streak voltage of 1000 V.

Images were corrected for the time delay associated with the vertical propagation of the excitation pulse through the cell. Decay curves were generated by summing down the image, typically 60−70 pixel rows high. Decay curves were also generated by summing the top 10 pixel rows and the bottom 10 pixel rows. These curves were compared to each other to assure that the shape of the signal was constant. From consideration of the overall intensity of the pump pulses and the similarity of the fluorescence signal from the top and bottom of the cell, it is clear that singlet−singlet annihilation effects do not contribute to the observed signal.

A single frame on the streak camera CCD provides a time window of approximately 90 ps. Additional time windows were obtained by delaying the synchronization pulse a precisely determined amount. Decay curves were obtained over total time windows of 140−300 ps. The precision of long time scale measurements with the current experimental arrangement is substantially less than that obtained in single photon counting measurements. As a result, we have concentrated on the determination of fast decay or rise components in the Q_y fluorescence. The 4−9 ps fwhm intrinsic instrument response and signal-to-noise ratio of the present experimental configuration are sufficient to permit good amplitude and rate constant analysis of kinetic components >2 ps. To allow accurate deconvolution of kinetic components, ca. 1−4 ps, an instrument response function was obtained from laser scattering for each set of measurements and used to fit the data.

Results

Spectral congestion present in the Q_y region of PSII precludes direct excitation of any individual pigment in the reaction center complex (see Figure 2). At room temperature the Q_y spectra of Chl and Pheo have bandwidths comparable to the bandwidth of the Q_y transition of the PSII reaction center complex. Thus,

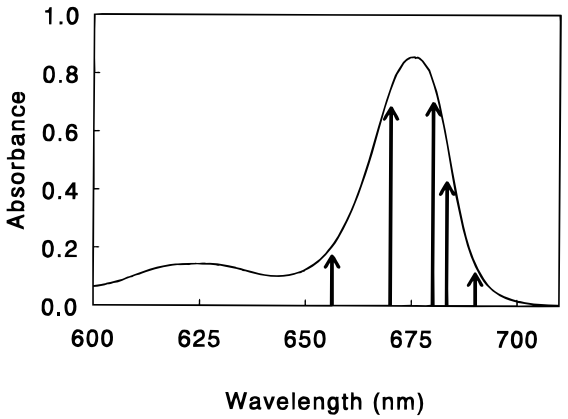

Figure 2. Absorption spectrum of D1−D2−Cyt b559 reaction center complex at room temperature. The arrows indicate the center wavelength for the excitation pulses used in the fluorescence measurements.

it is difficult to separate the contribution of individual molecules and investigate their roles in energy and electron transfer. The primary charge separation process leads to the formation of a hole in the absorption spectrum centered at 680 nm, which corresponds to bleaching of both the Chl donor (P680) and the Pheo acceptor. The width of the hole (ca. 13−14 nm at 100 ps[17]) is comparable to the width of the Q_y absorption band of the isolated Chl and Pheo pigments indicating that both the Chl and Pheo involved in the initial charge separation process have strongly overlapping absorption bands at 680 nm. No more detailed information is obtained from the room temperature spectrum. This spectral congestion greatly complicates the interpretation of time-resolved measurements in PSII. The specific initial distribution of reaction center excited states prepared with any given excitation pulse is determined by the spectrum of the pulse and the as yet unknown spectral composition of the PSII reaction center absorption band.

The situation improves somewhat under low-temperature conditions (<77 K). The bandwidths of Chl and Pheo are decreased to 5−8 nm, whereas for the reaction center the width is still 22−25 nm. Under these conditions the Q_y band is partially resolved, allowing identification of short-wavelength Chl having maxima at ∼672 nm and a long-wavelength form located at 680−683 nm.[18−20] Kinetic measurements and hole-burning measurements[8,21] at low temperature reveal a strong hole at 680 nm and a weak hole at 669 nm. The 680 nm hole represents bleaching of both the Chl and Pheo in production of the ion pair, while the hole at 669 nm is interpreted as the upper exciton band of a P680 Chl dimer.

Several attempts have been made to decompose the Q_y absorption band further.[22−24] Konermann and Holzwarth have recently published a detailed decomposition at low temperatures based on the hypothesis that the reaction center contains a P680 dimer of Chl molecules, while the remaining pigments are monomeric.[24] In this decomposition, P680, the active Pheo, and an additional Chl pigment contribute to the red (680−683 nm) absorbing pigment pool. The upper dimer transition of P680, the inactive Pheo, and three additional Chl contribute to the blue (ca. 670 nm) absorbing pigment pool.

An alternative model has been put forth by Durrant et al. with the excited states of at least six of the eight pigments coupled in a multimer.[25] The multimer states are further distinguished as being localized on the active branch or the inactive branch (two Chl and one Pheo in each branch). The remaining two weakly coupled Chl have absorption maxima at 670 and 675 nm.[14,25]

In the present set of measurements we have used excitation pulses centered at 656, 670, 680, and 690 nm (fwhm 10 nm)

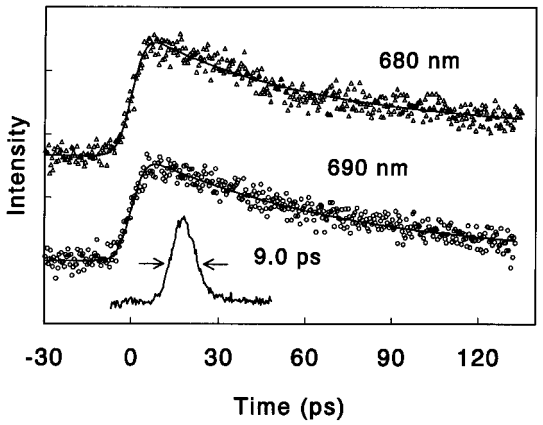

Figure 3. Fluorescence decay kinetics observed at 680 and 690 nm following excitation with a 656 nm excitation pulse. The experimentally determined instrument response function is also shown. The solid line through the fluorescence decays are the exponential fits to the data as discussed in the text.

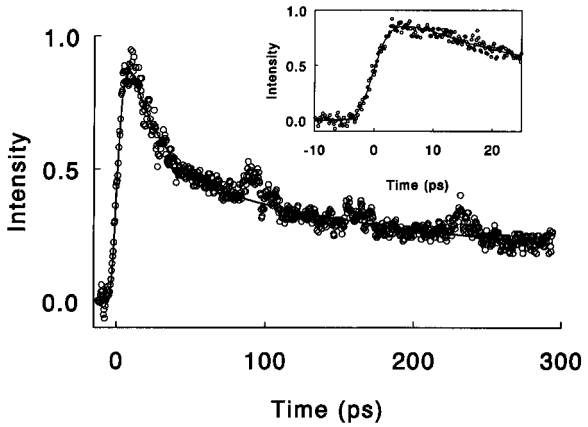

Figure 4. Fluorescence decay curve collected following excitation at 670 nm. Fluorescence was collected with a streak voltage of 408 V at four different synchronization delays for a total time window of ca. 300 ps. An additional data set, shown in the inset, was obtained with the streak voltage set at 819 V. The solid line is the exponential fit to the data as discussed in the text.

and a pulse at 683 nm (fwhm 3 nm). The 680 and 683 nm pump pulses were used to excite the primary donor P680 with as much selectivity as possible. Most models for the Q_y absorption band suggest that excitation at 680 nm will result in 25−35% direct excitation of P680. The overall selectivity for excitation of the redox active pigments, P680 and Pheo, should be at least 40−50%. This selectivity may be higher if the multimer model for PSII is valid. Excitation pulses centered at 670 and 656 nm were used to excite the Chl pigments absorbing on the blue edge of the Q_y band with some selectivity. Fluorescence was collected using a 10 nm band-pass filter centered at 690, 691, or 694 nm. This detection wavelength range was chosen to selectively probe the fluorescence from P680 inasmuch as possible. Following excitation at 656 nm the fluorescence was also analyzed using a 10 nm interference filter centered at 680 nm.

An additional fluorescence measurement was made with excitation at 690 nm to provide more exclusive excitation of the red absorbing pigments. Because of interference from scattering the fluorescence was detected at 670 nm, a wavelength which probes the population of the blue absorbing Chl. This is a particularly informative measurement.

656 nm Excitation. Fluorescence observed at 680 and 690 nm following excitation at 656 nm was time-resolved over a window of 150 ps (see Figure 3). The instrument function for this measurement was nearly a symmetric Gaussian with a fwhm of 9.0 ps. The fluorescence observed at 680 nm exhibits an instrument limited rise followed by a biexponential decay of 38 ± 5 and 170 ± 25 ps as well as a nondecaying component. The fluorescence observed at 690 nm exhibits an instrument limited rise followed by an exponential decay of 70 ± 10 ps and a nondecaying component. There is no evidence for a delayed rise of the fluorescence at these wavelengths. With the available instrument function and signal-to-noise ratio a fast (<2 ps) rise component cannot be excluded. However, inclusion of a rise of 1−2 ps increases the χ_R^2 value, and inclusion of a dominant rise component longer than 2 ps is visibly inconsistent with the data.

The 690 nm fluorescence may also be fit using a biexponential decay with time constants as found for detection at 680 nm although such a fit does not improve the χ_R^2 value. Clearly, the signal-to-noise ratio of the data set is not sufficient to distinguish definitively between a single-exponential, biexponential, or multiexponential decay for either detection wavelength. In fact, in this case and in every case where a reasonable comparison is possible, the data presented in this paper are compatible with the long (>10 ps) components obtained from TCSPC measurements.[7] Although the quality of the present data does not warrant a multiexponential analysis, curves calculated using the parameters available in ref 7 differ from the observed data only at early times.

670 nm Excitation. The fluorescence observed at 690 nm following excitation at 670 nm was time-resolved by using two different streak voltages. Fluorescence was collected with a streak voltage of 408 V at four different synchronization delays for a total time window of ca. 300 ps (Figure 4). An additional data set, shown in Figure 4 (inset), was obtained with the streak voltage set at 819 V.

These data were fit to a functional form consisting of a sum of three exponentials. The time window available in the present experiment was insufficient to determine time constants greater than ca. 200 ps. Therefore, the longest time constant was held fixed at 5 ns, a value chosen for consistency with the long time constant observed in single photon counting measurements.[5,7] The fit is not sensitive to the precise value of the longest rate constant. Time constants of 19 ± 1 and 200 ± 30 ps were determined for the two shorter decay components, consistent with values reported in the literature.[7]

The data support the possibility of a fourth, faster component. In order to deconvolute this component from the data, the three long components were held constant while a fourth much faster decay component was added and optimized. The asymmetric instrument response function (4.5 ps fwhm) used to analyze the data was obtained from the laser scattering signal under experimental conditions. Because the fast decay time component is obtained through deconvolution, the magnitude and time-constant are strongly correlated. The results of the fitting are summarized in Figure 5. The inclusion of a fast component results in an improved fit to the data as measured by the χ_R^2 value. However, the χ_R^2 curve as a function of τ_{short} is fairly shallow, and the presence of a short component cannot be considered a certainty.

680 nm Excitation. Fluorescence decays at 691 and 694 nm were analyzed following excitation at 680 nm. The fluorescence decay at 691 nm was obtained over a time window of 50 ps with an instrument response of 4.5 ps fwhm (Figure 6). The fluorescence decay at 694 nm was obtained over a time window of 140 ps with an instrument response of 9 ps fwhm (Figure 7). The overall decay of the fluorescence is substantially slower than the decay observed following excitation at 670 nm. The fluorescence decay at 694 nm was fit to a triexponential

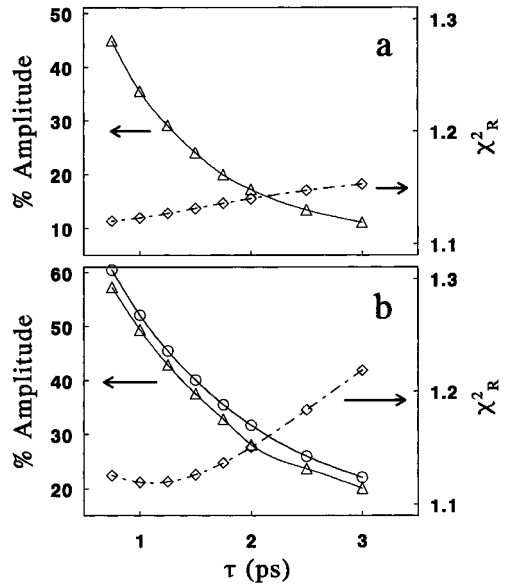

Figure 5. Comparison of the reduced χ^2 value and the magnitude of the short component as a function of the time constant for the data obtained following excitation at 670 (a) and 680 nm (b). The long component in the 680 nm data was modeled as a single 88 ps decay (circles) or a biexponential decay of 35 and 300 ps (triangles). The single-exponential long decay is all that is required by the limited time window in the data set (see Figure 6), while the biexponential long decay is used for consistency with the observed decay at 694 nm following excitation at 680 nm (see Figure 7). The absolute value of the minimum of the χ_R^2 curve changes with model for the long components, but the shape of the curve is unaffected. The χ_R^2 data shown correspond to an 88 ps decay plus a fast component.

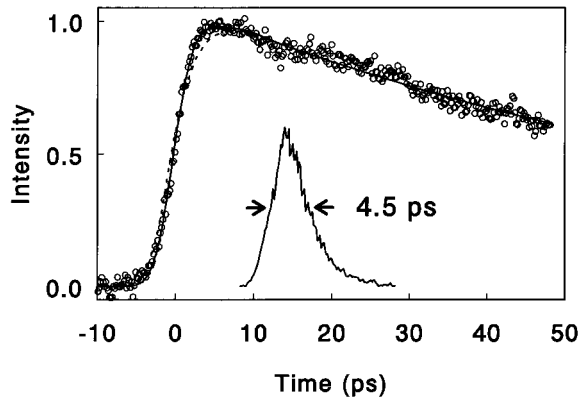

Figure 6. Fluorescence at 691 nm following excitation at 680 nm. These data were obtained over a time window of 60 ps with a streak voltage of 800 V. The solid line is the exponential fit to the data as discussed in the text. The dashed line is the best fit obtainable when neglecting the fast decay component. The data clearly require a fast component. The experimental instrument response function is also shown in this figure.

decay with the longest time constant held at 5 ns. The other two components obtained in the fit are 38 ± 5 and 300 ± 100 ps. The longer component is not well-defined due to the noise in the data and the limited time window. In addition, the data obtained following excitation at 680 nm with detection at 691 nm require a fast decay component. To analyze for this component, the long time components were held fixed while an additional much faster decay component was added and optimized. Figure 5b shows the results for the two different models for the long decay at 691 nm. In both cases the χ_R^2 curve as a function of τ_{short} exhibits a distinct minimum, and the optimal fit is found with τ_{short} = 1.0−1.25 ps, accounting

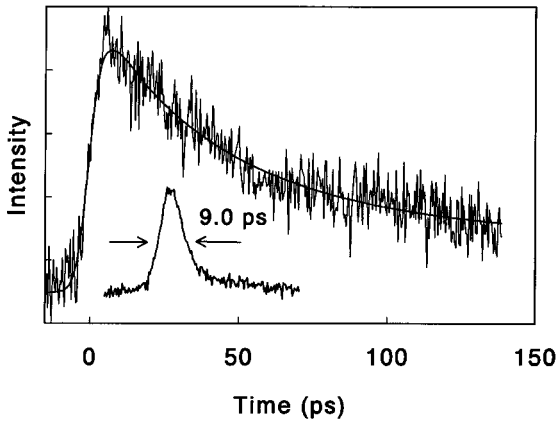

Figure 7. Fluorescence at 694 nm following excitation at 680 nm. These data were obtained over a time window of 150 ps. The smooth line through the data represents the exponential fit as discussed in the text. The experimental instrument response function is also included in the figure.

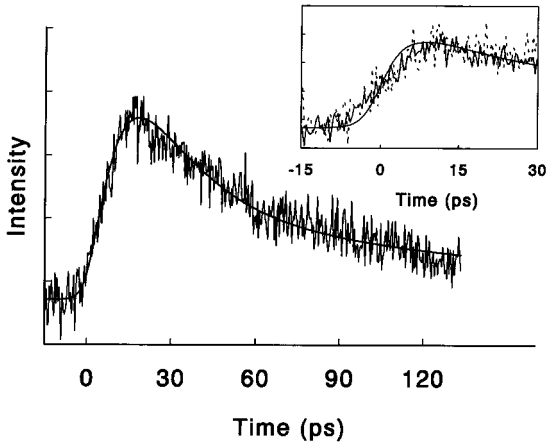

Figure 8. Fluorescence at 670 nm following excitation at 690 nm. The instrument response function for this data (not shown) had a 7.7 ps fwhm. The smooth line through the data represents the exponential fit as discussed in the text. The inset contains a comparison of two independent data sets obtained on different days with the best fit assuming an instrument limited rise and a monotonic decay. The data are visibly inconsistent with an instrument limited rise.

for 45−50% of the fluorescence decay. The limitations of the deconvolution procedure do not preclude the possibility that the short component is less than 1 ps. The data at 694 nm also require a fast decay component, although it is much less well-defined by this data set. The optimal fit is found with τ_{short} = 1.5−1.75 ps, again accounting for ca. 50% of the fluorescence decay.

A fluorescence decay over one time window (ca. 50 ps) was obtained following excitation with a 3 nm fwhm pulse centered at 683 nm. The instrument response function was 7 ps fwhm. These data (not shown) are also visibly inconsistent with a 3 ps decay of large amplitude (>33%). The quality of the present data is insufficient for a more detailed analysis.

690 nm Excitation. A fluorescence decay at 670 nm was obtained following excitation at 690 nm (Figure 8). This signal is quite weak, consistent with "uphill" energy transfer to the fluorescing pigments. As a result, the data are rather noisy. The inset in Figure 8 compares two distinct measurements (i.e., different days) of the 670 nm fluorescence with the best fit to an instrument limited rise. The observed fluorescence rise is clearly not instrument limited. The signal exhibits an 8 ± 1 ps rise followed by a 20 ± 3 ps decay, a 175 ± 25 ps decay, and a nondecaying component.

Discussion

There are several key observations in the data and analysis discussed above. These observations provide a severe constraint for any model of energy transfer and charge separation in PSII. In the discussion which follows the term reaction center core will be used to refer to P680 and that group of pigments coupled to P680 via rapid (<1 ps) energy transfer. The D1−D2−Cyt b559 complex may contain one or more additional pigment pools (a "pool" consists of one or more Chl or Pheo) coupled to the reaction center core via slow (>1 ps) energy transfer.

The data exhibit a slow multiexponential decay in the fluorescence intensity. The long overall fluorescence decay demonstrates that the initial charge separation step (or steps) involves a modest decrease in the free energy. A substantial portion of the population remains distributed over the excited electronic states for tens to hundreds of picoseconds. This is in distinct contrast to the reaction centers in purple bacteria where the excited state population is drained in the initial charge separation step on a dominant time scale of 3 ps.[26] Assuming that the D1−D2−Cyt b559 reaction center complex is a reliable model for intact PSII, the first unidirectional energy trap at room temperature (ca. 280 K) occurs in the secondary electron transfer from pheophytin to quinone on a 250 ps time scale.[27] This observation, although not unique to the present study (see for example refs 6 and 7), is not always properly appreciated. The observed rate constants must be interpreted in terms of equilibration processes, and the intrinsic charge separation rate constant can only be estimated on the basis of the data by using kinetic models.

Excitation on the red edge (690 nm) results in the delayed appearance of blue (670 nm) fluorescence. The rise time is ca. 8 ps. On the other hand, excitation at 656 nm results in prompt fluorescence at 680 and 690 nm followed by a relatively slow monotonic decay. These observations are in direct contrast to the kinetics obtained by deconvolution of TCSPC measurements which suggest a delayed rise of red fluorescence following excitation between 620 and 671 nm and a prompt rise of blue fluorescence following excitation at 686 and 689 nm.

The slow decay of the fluorescence following excitation at 656 nm is consistent with the presence of one or more blue absorbing chlorophyll coupled by slow energy transfer to the reaction center core. Such a model for PSII has been suggested repeatedly on the basis of transient absorption measurements.[1−3,8,28] However, the prompt red fluorescence also demonstrates that much of the excitation at 656 nm results in rapid energy transfer to "red" pigments or in direct excitation of "red" pigments via the high-energy wing of the absorption bands.

A more quantitative analysis of the slow energy transfer is possible based on the observed fluorescence at 670 nm. Excitation at 690 nm on the red edge of the Q_y band results in an average 8 ps rise for the population of the "blue" pigments (ν_{max} < 670 nm). Little if any population of the "blue" pigments occurs promptly. In a very simple three-level model consisting of a pool of "blue" pigments, a pool of "red" pigments comprising the reaction center core, and a charge-separated state, the observed rate of $(8 \pm 1 \text{ ps})^{-1}$ corresponds to the effective rate constant for "downhill" energy transfer from the "blue" pool to the reaction center core. (Equilibrium is established on a time scale determined by the sum of the rate constants.) The observed rise sets an upper limit for the rate of energy transfer from the majority of the "blue" pigments to the reaction center core.

The present data are inconsistent with a large 2−4 ps decay component following excitation at any wavelength. At all wavelengths reported here the most obvious kinetic components are ≥20 ps. However, a fast, ca. 1 ps, component is required to model the fluorescence decay obtained following excitation at 680 nm. A somewhat smaller fast component may also be present following excitation at 670 nm. This component may be associated with *effective* charge separation from the P680 pool of pigments as a sum of all equilibrium processes, i.e., charge separation and energy transfer, which reduce the population of P680 following direct excitation. However, use of the term "effective charge separation" or even "apparent charge separation" for the fast component is specious. The effective time constant is almost certainly dominated by a sum of intrinsic energy transfer processes rather than by the intrinsic charge separation rate constant.

Conclusions

Time-resolved fluorescence measurements have been performed on PSII using a state-of-the-art synchronized streak camera. The 4−9 ps instrument response function of this camera allows accurate determination of fast decay/rise components in the Q_y fluorescence. In every case where a reasonable comparison is possible, the data presented in this paper are compatible with the long (>10 ps) components obtained from TCSPC measurements.[7] Curves calculated using the parameters available in ref 7 differ from the observed data only at early times.

The present data are inconsistent with an effective or an apparent charge separation time scale of ca. 3 ps following direct excitation of P680. No population decay component in the 2−4 ps range is observed for any combination of excitation and emission wavelengths. Rather, the effective charge separation from a quasi-equilibrium of chromophore excited states is either quite fast (≤1.25 ps) or relatively slow (≥20 ps).

The most consistent interpretation of the available data involves rapid energy redistribution processes within pools of pigments, somewhat slower energy redistribution between pools of pigments, and relatively slow multiexponential charge separation from a progressive quasi-equilibrium of pigment excited states. Such a model may be consistent with a ca. 3 ps intrinsic charge separation time scale. A more precise model for energy transfer and charge separation in PSII awaits a global analysis of more extensive fluorescence measurements.

Acknowledgment. Support for this research was provided by a grant from the National Science Foundation (MCB-9418390) and the Cindy Yoder Research Award of the University of Michigan to R.J.S. C.F.Y. was supported by NSF (MCB-9314173) and USDA-NCGRIP-96-35306-3399. We also acknowledge the assistance of the Center for Ultrafast Optical Science (NSF PHY-9319017).

References and Notes

(1) Klug, D.; Rech, T.; Joseph, M. D.; Barber, J.; Durrant, J. R.; Porter, G. *Chem. Phys.* **1995**, *194*, 433.

(2) Muller, M.; Hucke, M.; Reus, M.; Holzwarth, A. R. *J. Phys. Chem.* **1996**, *100*, 9527.

(3) Greenfield, S. R.; Seibert, M.; Govindjee; Wasielewski, M. R. *Chem. Phys.* **1996**, *210*, 279.

(4) Donovan, B.; Walker, L. A. II; Yocum, C. F.; Sension, R. J. *J. Phys. chem.* **1996**, *100*, 1945.

(5) Booth, P. J.; Crystall, B.; Ahmad, I.; Barber, J.; Porter, G.; Klug, D. *Biochemistry* **1991**, *30*, 7573.

(6) Freiberg, A.; Timpmann, K.; Moskalenko, A. A.; Kuznetsova, N. Y. *Biochim. Biophys. Acta* **1994**, *1184*, 45.

(7) Gatzen, G.; Muller, M.; Griebenow, K.; Holzwarth, A. R. *J. Phys. Chem.* **1996**, *100*, 7269.

(8) For reviews see: Greenfield, S. R.; Wasielewski, M. R. *Photosyn. Res.* **1996**, *48*, 83. Van Grondelle, R.; Dekker, J. P.; Gillbro, T.; Sundström, V. *Biochim. Biophys. Acta* **1994**, 1187, 1. Seibert, M. In *The Photosynthetic Reaction Center*; Deisenhofer, J., Norris, J. R., Eds.; Academic Press: San Diego, 1993; p 319.

(9) Muller, M. G.; Hucke, M.; Reus, M.; Holzwarth, A. R. *J. Phys. Chem.* **1996**, *100*, 9537.

(10) Ghanotakis, D. F.; de Paula, J. C.; Demetriou, D. M.; Bowbly, N. R.; Peterson, J.; Babcock, G. T.; Yocum, C. F. *Biochim. Biophys. Acta* **1988**, *974*, 44.

(11) Dekker, J. P.; Bowbly, N. R.; Yocum, C. F. *FEBS Lett.* **1989**, *254*, 150.

(12) Kwa, S. L. S.; Newell, W. R.; van Grondelle, R.; Dekker, J. P. *Biochim. Biophys. Acta* **1992**, *1099*, 193.

(13) Schelvis, J. P. M.; van Noort, P. T.; Aartsma, T. J.; van Gorkom, H. J. *Biochim. Biophys. Acta* **1994**, *1184*, 242.

(14) Merry, S. A. P.; Kumazaki, S.; Tachibana, Y.; Joseph, M. D.; Porter, G.; Yoshihara, K.; Barber, J.; Durrant, J. R.; Klug, D. R. *J. Phys. Chem.* **1996**, *100*, 10469.

(15) Demiodov, A.; Donovan, B.; Walker, L. A. II; Yocum, C. F.; Sension, R. J. Manuscript in preparation.

(16) Maksimchuk, A.; Kim, M.; Workman, J.; Korn, G.; Squier, J.; Du, D.; Umstader, D.; Mourou, G.; Bouvier, M. *Rev. Sci. Instrum.* **1996**, *67*, 697.

(17) Vacha, F.; Joseph, D. M.; Durrant, J. R.; Telfer, A.; Klug, D. R.; Porter, G.; Barber, J. *Proc. Natl. Acad. Sci. U.S.A.* **1995**, *92*, 2929.

(18) Van Kan, P. J. M.; Otte, S. C. M.; Kleinherenbrink, F. A. M.; Nieveen, M. C.; Aartsma, T. J.; van Gorkom, H. J. *Biochim. Biophys. Acta* **1990**, *1020*, 146.

(19) Otte, S. C. M.; van der Vos, R.; Gorkom, H. J. *J. Photochem. Photobiol. B: biol.* **1992**, *15*, 5.

(20) Mimuro, M.; Tomo, T.; Nishimura, Y.; Yamazaki, I.; Satoh, K. *Biochim. Biophys. Acta* **1995**, *1232*, 81.

(21) Groot, M. L.; Dekker, J. P.; van Grondelle, R.; den Hartog, F. T. H.; Volker, S. *J. Phys. Chem.* **1996**, *100*, 11488.

(22) Van Dorssen, R. J.; Breton, J.; Plijter, J. J.; Satoh, K.; van Grokom, H. J.; Amesz, J. *Biochim. Biophys. Acta* **1987**, *893*, 267.

(23) Braun, P.; Greenberg, B. M.; Scherz, A. *Biochemistry* **1990**, *29*, 10376.

(24) Konermann, L.; Holzwarth, A. R. *Biochemistry* **1996**, *35*, 829.

(25) Durrant, J. R.; Klug, D. R.; Kwa, S. L. S.; van Grondelle, R.; Porter, G.; Dekker, J. P. *Proc. Natl. Acad. Sci. U.S.A.* **1995**, *92*, 4798.

(26) Du, M.; Rosenthal, S. J.; Xie, X.; DiMagno, T. J.; Schmidt, M.; Hanson, D. K.; Schiffer, M.; Norris, J. R.; Fleming, G. R. *Proc. Natl. Acad. Sci. U.S.A.* **1992**, *89*, 8517.

(27) Rutherford, A. W. In *Light Energy Transduction in Photosynthesis: Higher Plants and Bacterial Models*; Stevens, S. E., Bryant, D., Eds.; American Society of Plant Physiologists: Rockville, MD, 1988; pp 163−177.

(28) Holzwarth, A. R.; Muller, M. G.; Gatzen, G.; Hucke, M.; Greibenow, K. *J. Lumin.* **1994**, *60&61*, 497.